Full Paper

Wiley Online Library

ELECTROANALYSIS

DOI: 10.1002/elan.201900435

Evaporation of Electrolyte during SVET Measurements: The Scale of the Problem and the Solutions

A. C. Bouali,*[a] A. C. Bastos,[b] S. V. Lamaka,[a] M. Serdechnova,[a] M. G. S. Ferreira,[b] and M. L. Zheludkevich[a, c]

Abstract: The objective of this work is to investigate the scale of the effect of spontaneous solution evaporation during SVET (Scanning Vibrating Electrode Technique) measurements and demonstrate how it biases the final results. When SVET maps are continuously acquired for more than several hours, the measured currents are smaller than expected. This is attributed to solvent (typically water) evaporation which leads to an increase in solution conductivity over time. If this is not considered when converting the measured potential differences into the local current densities, the SVET results display currents smaller than the true ones. Here, this effect is studied with a platinum disk electrode as source of a constant current and a model corroding system consisting of the AA2024/CFRP galvanic couple. Corrective actions are proposed to mitigate the problem, either in the experimental set-up or as numerical correction.

Keywords: SVET · scanning vibrating electrode technique · solution evaporation · conductivity

1 Introduction

The scanning vibrating electrode technique (SVET) is an efficient tool to investigate localized corrosion occurring on different metallic surfaces [1–10]. Recently, it has been actively used for monitoring the activities in the defects of self-healing coatings. SVET measurements are carried out in aqueous electrolyte using a vibrating probe maintained at a certain distance from the surface. Often, SVET measurements last for 24 hours or longer [11–13]. The microelectrode registers an alternating potential at the vibration frequency that is proportional to the electric field strength in the direction of vibration, which in turn is proportional to the local current density flowing in the point of measurement according to,

$$j = \kappa E \quad (1)$$

where j is the local current density, κ is the solution conductivity and E is the electrical field in the point of measurement.

There are a number of operation parameters and factors that need to be taken into account when using this technique in order to obtain accurate data and avoid artifacts. Many studies have been performed to optimize the SVET from both theoretical and experimental standpoints [14–25]. The technique is assumed to not interfere with the sample or with the corrosion process. However, McMurray *et al.* highlighted the effect of large amplitude probe vibrations on the electrochemical processes taking place on the specimen surface, especially when oxygen diffusion is the rate-determining step [17]. It was verified that cathodic activity beneath the probe tends to increase linearly with large vibration amplitudes leading to an overestimation of the local cathodic currents. In a recent work, this issue was revisited with a different probe and cell geometry, similar to those used in this work. It was concluded that under normal operating conditions the vibration does not affect the measurement, contrarily to the probe movement which can facilitate the transport of dissolved oxygen to the surface, thus momentarily increasing the cathodic activity [23].

The SVET results can also be affected by the change of global or local electrolyte concentration during the measurement. One of the origins of such change of the concentration is uncompensated solvent evaporation in continuous long-term experiments. The consequent increment of the electrolyte conductivity leads to current values smaller than the true ones, if not taken into

[a] A. C. Bouali, S. V. Lamaka, M. Serdechnova, M. L. Zheludkevich
Institute of Materials Research, Helmholtz-Zentrum Geesthacht, Max-Planck-Straße 1, Geesthacht 21502, Germany
Tel./Fax: +49 4152 87-1943/ 1960
E-mail: anissa.bouali@hzg.de
[b] A. C. Bastos, M. G. S. Ferreira
CICECO-Aveiro Institute of Materials and DEMaC-Department of Materials and Ceramic Engineering, Universidade de Aveiro, 3810-193 Aveiro, Portugal
[c] M. L. Zheludkevich
Faculty of Engineering, Kiel University, Kaiserstraße 2, Kiel 24143, Germany

account when converting the measured potential differences into the local current densities.

This is critical for all applications, but especially for numerical modelling when the actual experimental data are compared with the simulated results. It is also crucial in studies dealing with the self-healing properties of coatings and corrosion inhibition. In both cases, efficient systems are associated with the decrease of the ionic currents in solution detected by SVET. However, it is imperative that the decrease in SVET currents comes only from the sample and not from an experimental artifact introduced by the electrolyte evaporation during the measurement. Some SVET apparatuses are relatively immune to this problem because the electrochemical cells have large compartments for the electrolyte solution [4,17,19,21,26–27], but others, including the one employed in the present work, use small volumes, of the order of a few milliliters.

Although this problematic is apparent, it is often neglected and not given enough attention. For instance, in most corrosion related studies involving SVET measurements authors do not explain the precautions taken to prevent or limit the evaporation of the test electrolyte during long-term SVET measurements [5–7,11–13,20,28–37].

In this work, the importance of solution evaporation was evaluated with SVET measurements performed during 24 hours on an AA2024/CFRP galvanic couple, followed by a more detailed study with a platinum disk driving a constant cathodic current.

2 Experimental

The SVET equipment used in this work was manufactured by Applicable Electronics Inc. [38] and controlled by the ASET program developed by Science Wares [39]. The measurements were performed using a Pt/Ir microelectrode with a tip in the form of a spherical platinum deposit of 20 μm diameter. The microelectrode vibrated at 117 Hz in the direction parallel to the surface and 70 Hz in the normal direction. The peak amplitude of vibration was 5 μm. Two different model samples were used to carry out the study. The first consisted of a galvanic couple composed by 2024 aluminum alloy rod (Alcoa, USA, nominal composition in wt.%: 4.55 Cu, 0.17 Fe, 1.49 Mg, 0.45 Mn, 0.10 Si, 0.02 Ti, 0.16 Zn, less than 0.01 Cr and Al balance) connected to aeronautical grade carbon fiber reinforced plastic rod (65 % Tenax HT 24 K carbon fiber in an epoxy vinyl matrix) both in an epoxy mount with the surface finished with SiC 1200 abrasive paper Figure 1a. The map comprised 3800×1800 μm^2 and the number of points was 91×51. In each point, the probe waited 0.05 second and measured for 0.05 seconds before moving to the next point.

The second model sample was a platinum wire of 250 μm diameter (99.99 %, Aldrich, 267171) vertically embedded in epoxy resin to form a disk shape upon grinding and connected to the current source of the SVET equipment (Figures 2a) and b). With this sample, a constant current of −60 nA was applied and maintained during the entire experiment. The map comprised 51×51 points with a scan area of 400×400 μm^2. The sampling rules were increased to 0.2 seconds waiting and 0.2 seconds measuring. In both cases, the distance to sample surface was of 100 ± 1 μm and the measurements were performed with 0.05 M NaCl, near neutral pH aqueous solution at room temperature (22 ± 2 °C). The diameter of the cell was 31.8 mm so that the surface area of the electrolyte is at least 7.94 cm^2 (not counting the distortion caused by the meniscus). The volume of the electrolyte in the cell was around 4 ml.

As a next step, two set-ups were proposed in an attempt to maintain constant the solution volume in the cell. One set-up was based on the principle of the communicating vessels. The test cell was connected through a pipe to 100 ml vessel containing the same solution (0.05 M NaCl). This will allow for the electrolyte volume in the cell to be balanced out during evaporation.

The other set-up relied on a continuous flow of solution between the test cell and a flask containing 400 ml of the same solution. This was achieved using a peristaltic pump where the flow rate was maintained at 10 ml/min. A scheme for both set-ups is provided further in the paper.

3 Results and Discussion

3.1 The Impact of Solution Evaporation

To identify the impact of solution evaporation on the SVET measurements, the corrosion of a model CFRP-AA2024 galvanic couple was monitored every hour during the first day of immersion in 0.05 M NaCl. A galvanic couple with well separated anode and cathode was chosen to simplify the detection of changes in the current densities.

Optical images and SVET maps acquired after 1 hour and 24 hours are represented in Figure 1b)–e). A clear cathodic region corresponding to the CFRP is defined on the right side of the current maps whereas the AA2024 (on the left side) is characterized by localized corrosion with many anodic regions surrounded by small cathodic activity. A noticeable decrease in current density is observed from the first (1 h) to the last map (24 h), which suggests a reduction in corrosion rate with time.

The evolution of the total cathodic and anodic integrated current values (Figure 1g)) confirms this decrease of activity with time. Such an effect is expected in the presence of corrosion inhibitors, but this is not the case. Reasons for this decrease of current densities could be a partial blocking of the anode by corrosion products, providing some sort of protection to the AA2024, or a depletion of the oxygen concentration during long-term measurements. A more plausible explanation is the evaporation of the test solution, leading to an increase of the NaCl concentration. As a consequence, the solution

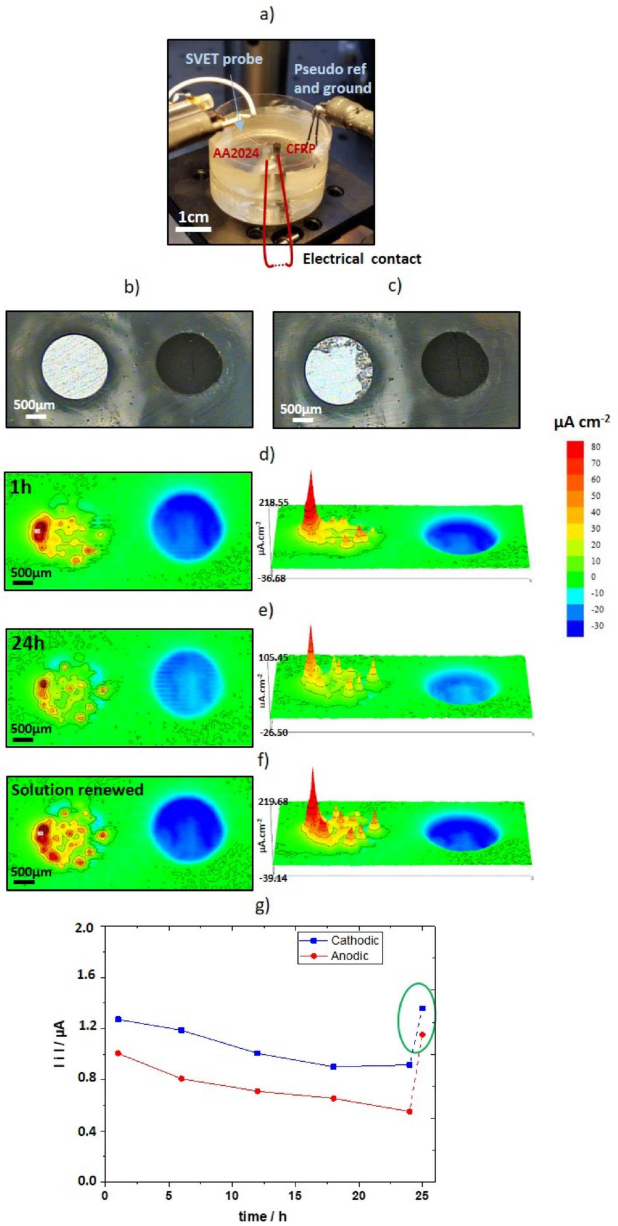

Fig. 1. a) Cell used for SVET measurements above a CFRP connected to AA2024 sample b) optical micrograph of the CFRP-AA2024 couple after 1 h of immersion, c) optical micrograph after 24 h of immersion, d) SVET maps (2D and 3D) of current density measured 100 µm above the surface after 1 hour; e) SVET maps measured after 24 hours ; f) SVET maps acquired after renewing the solution, g) integrated cathodic and anodic current values at different periods of time (1 h, 6 h, 12 h, 18 h and 24 h), and after renewing the solution.

conductivity gradually increases changing the original calibration conditions that were set at the beginning of the experiment. The result is a decrease of the current calculated by equation (1) compared to the real value. The last explanation was confirmed when the measurement at 24 hours of immersion was repeated after renewing the test solution (returning to the original calibration conditions). As depicted in Figure 1f), the current densities in the new map are very close to those in the map measured after 1 hour of immersion, the same applied to the integrated anodic and cathodic currents. This region is highlighted in green in the graphs of Figure 1g).

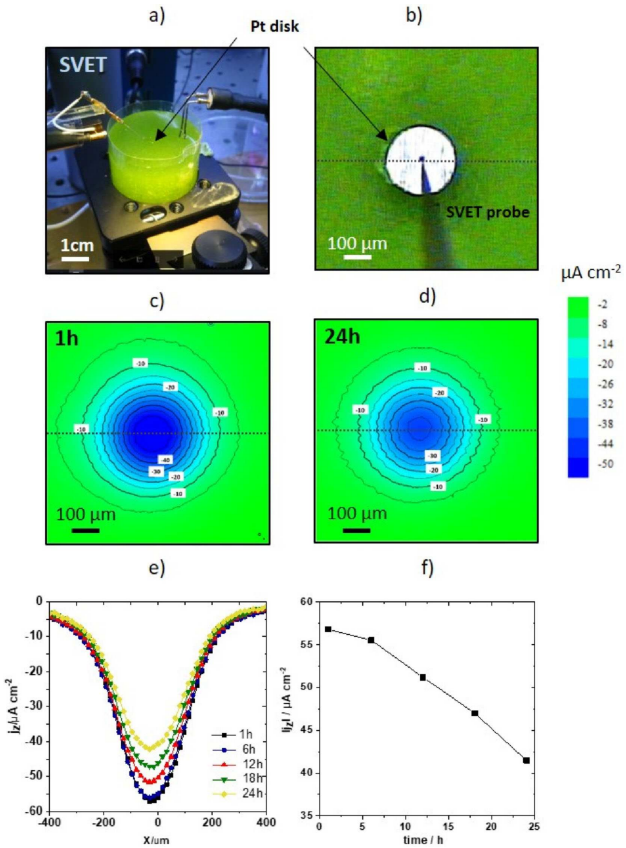

Fig. 2. a) Cell used for SVET measurements above a polarized Pt disk; b) 250 µm platinum disk as current source with vibrating probe above it; c) SVET map of current density measured 100 µm above Pt disk (I = −60 nA) after 1 hour; d) SVET map after 24 hours; e) Current density profiles obtained at selected hours through the middle of the Pt disk; f) Evolution of the peak current density vs. time of immersion.

3.2 Measurements with Platinum Disk as Current Source

A number of experiments was carried out with a platinum disk driving a constant current to understand better the origin of the effect. Figure 2 shows SVET maps obtained above the platinum disk, after, respectively, 1 hour and 24 hours of immersion. As in Figure 1, the maps show a decrease in current during the 24 hours period. Lines passing through the middle of the platinum disk at selected times of immersion and the maximum current in each line are presented in Figure 2e) and f) giving a clear illustration of the decrease in the measured current. Without considering the evaporation effect, these results are unexpected since the current at the source remained constant. Thus, the hypothesis on the decrease of the measured current on galvanic couple because of the potential depletion of oxygen concentration can be

rejected. A partial blocking of the platinum surface by fouling cannot explain the results as well since the power source would force the cell potential to keep the selected current constant. The evaporation of solution remains the most probable reason. It causes the increase of the conductivity and the decrease of the potential gradient needed to drive the same current flow following the Ohm's law. The SVET relates the measured potential differences with the local current densities using equation (1). For a constant current, where evaporation takes place, the conductivity increases and the potential in solution decreases proportionally. If both are taken into consideration in equation (1), the real current stays the same. However, the conductivity for the calibration is defined at the beginning of the test and remains unchanged. As a consequence, the resulting measured current densities decrease in time, while the constant current source remains the same.

In a corrosion study, the increase of conductivity without correction leads to a wrong estimation of the magnitudes of the current densities but does not change their polarities or the distribution of anodes and cathodes. It can lead to a false positive manifestation of a self-healing process when measurements are done above the active corroding defects in a coating. The decrease of solution volume (by water evaporation) also bring additional problems like changes of the medium corrosivity, pH, metal cation concentration and solubility of corrosion products, each alone capable of modifying the kinetics of the corrosion process.

3.3 Solution Evaporation Rate

In order to estimate the solution evaporation rate SVET maps were measured periodically, starting with the probe in air (out of solution), moving vertically and ending in a position well inside the solution. The absolute values of the measured currents do not matter in this case, but the signal measured by SVET is considerably different inside and outside the electrolyte, allowing the determination of the solution level at each moment of measurement. Figure 3 shows the maps obtained during a 24 hours period, putting in evidence the evaporation rate. The

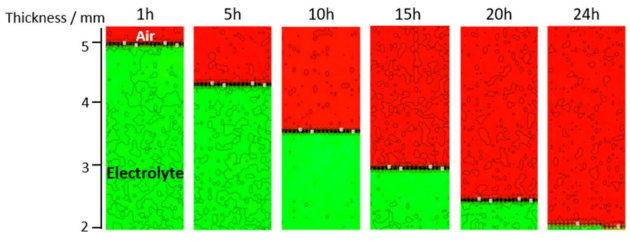

Fig. 3. SVET maps normal to the surface showing the decreasing level of the test solution over time (the starting height of solution was 5 mm, the lowest measured line was at 2 mm from the sample surface). In the maps the red area is outside the solution (air) and the green area is the electrolyte solution.

initial level of solution was 5 mm and decreased to 2 mm after 24 hours, a 60 % decrease. Obviously, the evaporation rate strongly depends on parameters such as air and electrolyte temperature, humidity, air velocity and gas/liquid contact area [40,41]. The values obtained in this paper are restricted to the conditions of local environment where the experiments were performed. In fact, repetitions in different days and parallel experiments in different locations led to different evaporation rates with the same exact electrochemical cells.

3.4 Correcting the Current Density by Updating the Bulk Conductivity

The measurements above a platinum disk with an applied current of −60 nA were repeated with the simultaneous assessment of the solution layer thickness at the time of each map acquisition. The layer thickness was measured using the same method described above to determine the evaporation rate. Figure 4a) shows the decrease of the solution thickness measured during 29 hours, which allows to calculate the volume of the solution, represented in the same figure, and then estimate the increase in concentration and instant conductivity both shown in Figure 4b).

The concentration at time t (C_t) is calculated knowing the initial volume (V_0) and concentration (C_0), the volume at time t (V_t) and using the relation ($C_0\ V_0 = C_t\ V_t$). The theoretical conductivity can be determined using the following equation [42]:

$$\kappa = F^2 \sum \frac{Z_i^2 D_i C_i}{RT} \tag{2}$$

where κ is the solution conductivity ($S\,cm^{-1}$), F is the Faraday constant ($96495\ C\,mol^{-1}$), R is the ideal gas constant ($8.314\ J\,K^{-1}\,mol^{-1}$), T is the absolute temperature (298 K for standard conditions), z_i and D_i are, respectively, the charge and diffusion coefficients ($cm^2\,s^{-1}$) of the species i in solution. The species considered were the sodium ion ($D_{Na+} = 1.33 \times 10^{-5}\ cm^2\,s^{-1}$) and the chloride ion ($D_{Cl-} = 2.03 \times 10^{-5}\ cm^2\,s^{-1}$) [43]. The ions OH^-(aq) and H^+(aq) were not considered because the solution has a (pH ≈ 6) and their bulk concentrations are below 10^{-6} M, bringing no effect to the calculation. The concentration C_i ($mol\,cm^{-3}$) was updated for each moment of measurement. The conductivity values were used for correcting the current densities measured in the maps obtained during the 29 hours testing period using,

$$j_{tc} = j_{tm}\ \kappa_t / \kappa_0 \tag{3}$$

where j_{tc} is the corrected current density at time t, κ_t is the solution conductivity estimated for time t, j_m is the measured current density at time t and κ_0 is the conductivity measured at the beginning of the tests.

Figure 5. shows the peak current density measured in each map during the experiment. The measured peak current densities represented in Figure 5 (in blue) are the

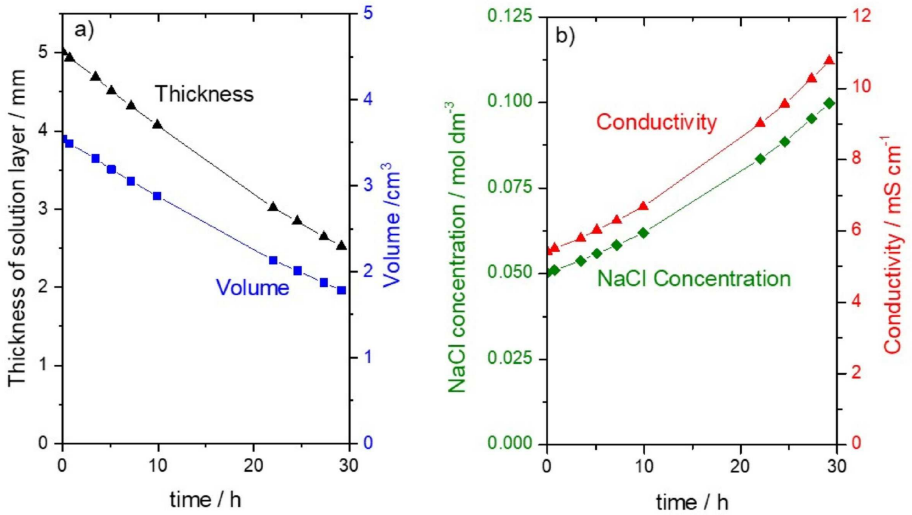

Fig. 4. Evolution during 29 hours of: a) measured thickness of solution layer and calculated solution volume in the SVET cell, b) estimated NaCl concentration and corresponding conductivity as a results of water evaporation.

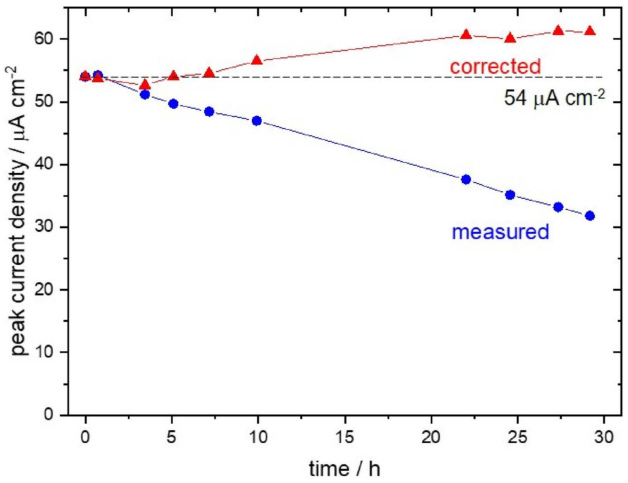

Fig. 5. Peak current density of maps measured during 24 hours at the condition of spontaneous solution evaporation and the same currents after correction with the conductivity calculated based on the measured evaporation rate.

ones obtained above a platinum disk with an applied current of −60 nA whereas the corrected curve in Figure 5 (in red) results from the corrections applied to it, using the conductivity values obtained earlier (Figure 4).

It is evident that while the total current at the platinum disk was constant (−60 nA) the measured current density was decreasing with the time of immersion. The correction using equation (3) is able to bring in the first hours, the current density back to the original value although with time an overcompensation is observed. This can be due to an inaccurate estimation of the solution volume which was based just on the height of the solution, not considering the meniscus formed around the walls of the solution reservoir and also a possible change of the diffusion constants as the concentration increases. As the height and volume of the electrolyte decrease, the contribution of the concave meniscus to the total volume of the electrolyte increases. The j_{tc} value of 61 µA cm^{-2} at 29 hours could turn into the "true" value of 54 µA cm^{-2} if the volume used for the correction was just 10 % higher (0.17 ml), easily accommodated in the meniscus.

Another factor to take into account is temperature. The solution conductivity is very sensitive to changes in temperature and an increase in 4 °C would suffice to bring the corrected current at 29 hours to the "true" value. Such a variation is too high to happen in laboratories with controlled room temperature. Nevertheless, smaller changes of all above parameters can align together to create conditions for the discrepancy observed between the true and the "corrected" values. The main conclusion is that the post treatment is possible but needs the control of a few parameters which makes it difficult to obtain a truly complete and reliable correction. Moreover, the evaporation profile is not universal. Different profiles were obtained with the same cells, confirming the importance of the local environment conditions.

3.5 Modified Cell to Prevent the Change in Concentration

Since the evaporation is a factor that may significantly affect the accuracy of the results, it is better to prevent it instead of making post-measurement corrections. A simple process is to renew the solution at specific intervals. However, this can wash away corrosion products, might change the surface condition and the forced convection may alter the natural slow evolution of the corrosion events.

Alternatively, water can be added dropwise until the initial level of solution is regained. This procedure works if carefully done but is not practical for overnight periods or long absence of the experimenter. Another way is to

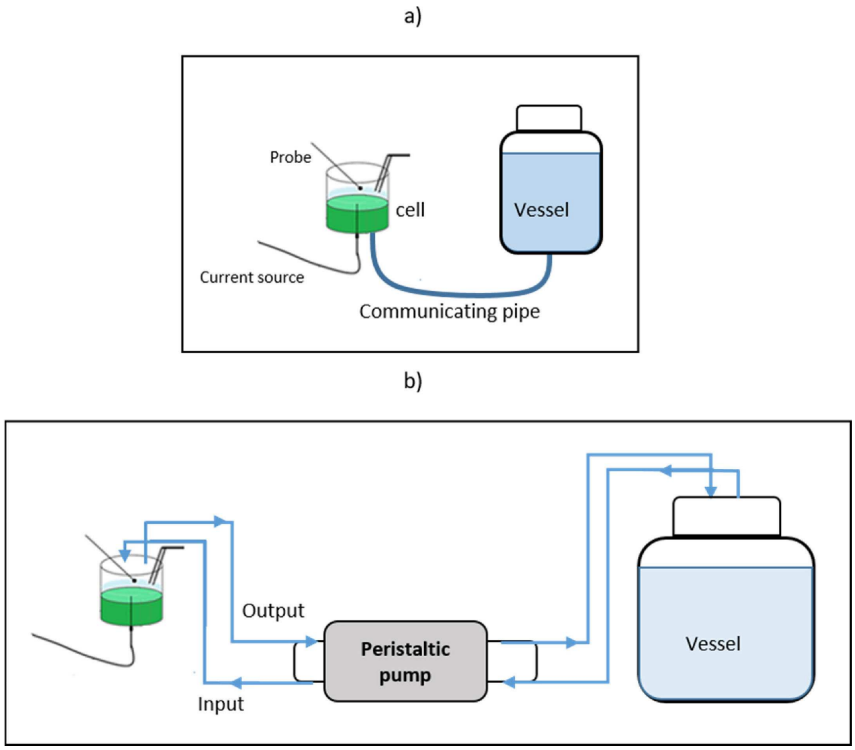

Fig. 6. Cell design to overcome the problem of evaporation: a) communicating vessels and b) a closed recirculating flow system using a peristaltic pump.

use larger cell compartments to increase the volume of the test solution.

A small cell can have its solution volume incremented by attaching a communicating vessel or setting-up a flow system connected to a large reservoir of solution. The two last methods have been tested and are sketched in Figure 6. The first set-up is based on the principle of two communicating vessels so that the volume of the solution does not decrease significantly during time. The second option relies on a continuous refreshing of the solution using a peristaltic pump.

3.6 Comparison of Post-correction and Modified Cells

Figure 7 compares the approaches just described to improve the results in Figure 2. Figure 7a1)–a3) is the same as Figure 2c)–e). Figure 7b1)–b3) shows the same data corrected using equation (3) and updated with the recalculated conductivity in each time of measurement.

Figures 7c1)–c3) show the experiment repeated with a communicating vessel set-up and Figures 7d1)–d3) show the measurements with a recirculating flow system. All of these procedures present improvements regarding the initial experiments presented in Figure 2 but the best results were obtained with the recirculating flow system, employing a peristaltic pump.

3.7 Measurement of the AA2024-CFRP Model Corroding System with the Continuous Flow Cell

The recirculating flow system, that minimizes the effect of spontaneous evaporation of the solution, was used to record once again the evolution of local current density of the AA2024-CFRP galvanic couple. The results are presented in Figure 8. Although a decrease of corrosion activity is still observed, it is much smaller than that observed in Figure 1d) and e).

Continuous circulation of corrosion medium significantly decreases the effect of spontaneous solution evaporation and decreases the chance for observing artifacts such as false-positive self-healing.

At the end of this paper two final remarks must be emphasized. The first is that evaporation is not always as evident and dramatic as it was described here. In this work very different evaporation rates were found in different days and in different places within the same day. The second is that not all SVET systems face this problem, which is easily minimized by using large compartments of the test solution. All in all, important is to prevent unwanted and oblivious concentration changes in SVET studies. Circulation of a large volume of solution, by e. g. a peristaltic pump, allows minimizing the effect of solution evaporation to non-detectable level. The flow rate of even below 0.01 ml/min is sufficient to maintain the concentration of the solution, while it is too low to influence the corrosion process [44]. On the other

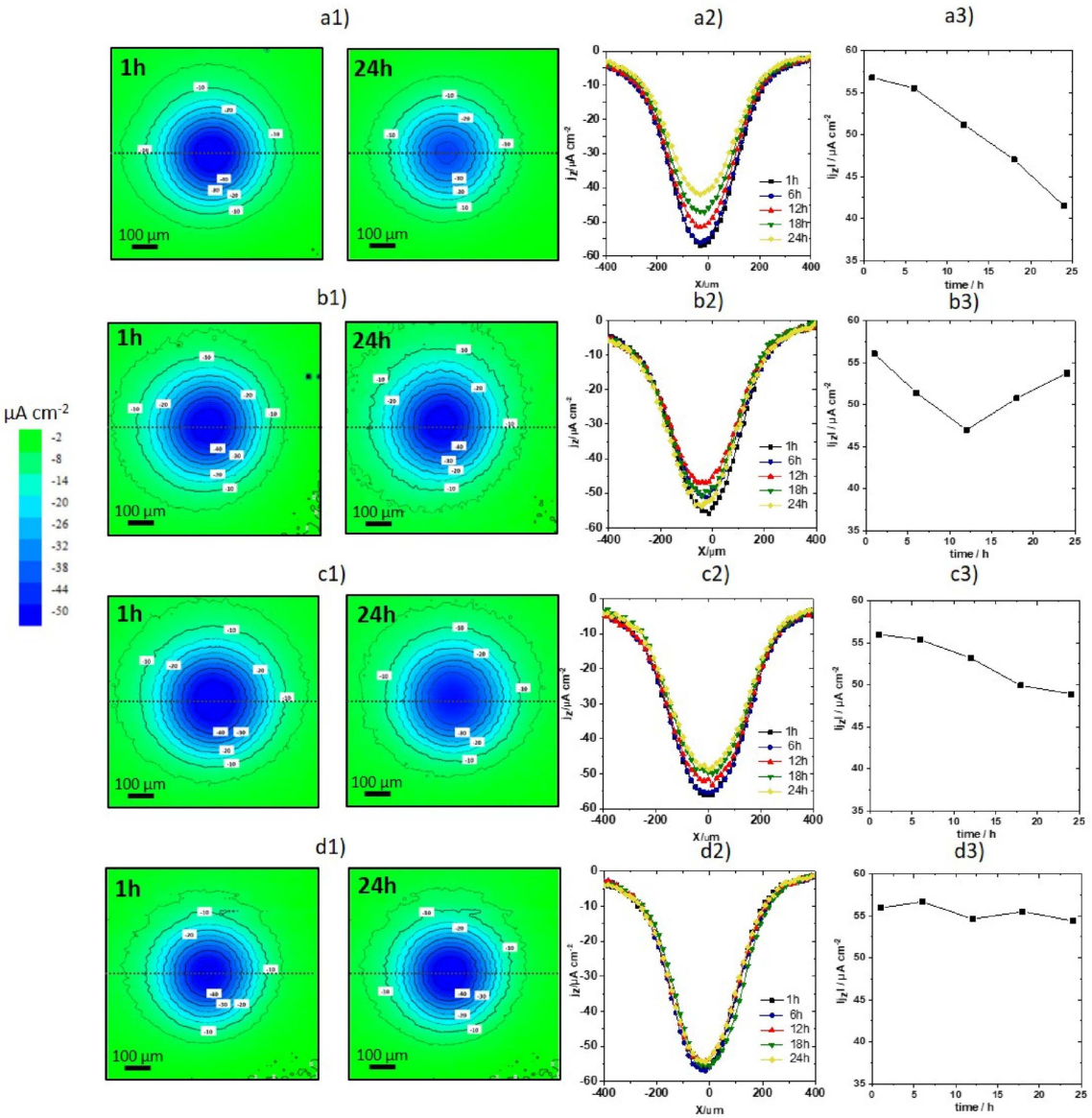

Fig. 7. Current density measurements (initial and after 24 hours) over Pt disk injecting constant current of −60 nA. a) Results affected by spontaneous evaporation without corrections (same as Figure 2 c)–d), shown here for direct comparison); b) Results presented in a) corrected using equation (3); c) Measurements obtained using the communicating vessels; d) Results obtained using a recirculating flow system with peristaltic pump. In a), b) and c), 1 is for maps, 2 is for current density profiles passing through the middle of te Pt disk and 3 is for the peak current density vs. time of immersion.

hand, even at the flow rate of as high as 1.5 ml/min, local pH, in the Nernstian diffusion layer can be clearly distinguished from the bulk values [45].

4 Conclusion

This work highlights the effect of spontaneous water evaporation on local current densities measured by SVET, which can be significant. Although this problem is obvious, it is not given sufficient attention in everyday experimenting. Increased concentration and conductivity of the electrolyte distort the current magnitudes, especially in the experiments lasting for more than just a few hours. Tests were conducted with a model galvanic couple and an inert platinum wire electrode driving a constant cathodic current.

In some experiments, in a period of 24 hours, a decrease in solution volume of 50 % was observed with a decrease in current density measured by SVET of the same order of magnitude. Such a decrease could be erroneously attributed to (false-positive) self-healing effect. The water evaporation rate leading to the decrease in solution volume and SVET current is not universal and depends on the local environment conditions.

Different ways to overcome this problem were discussed. The best approach relies on the use of a

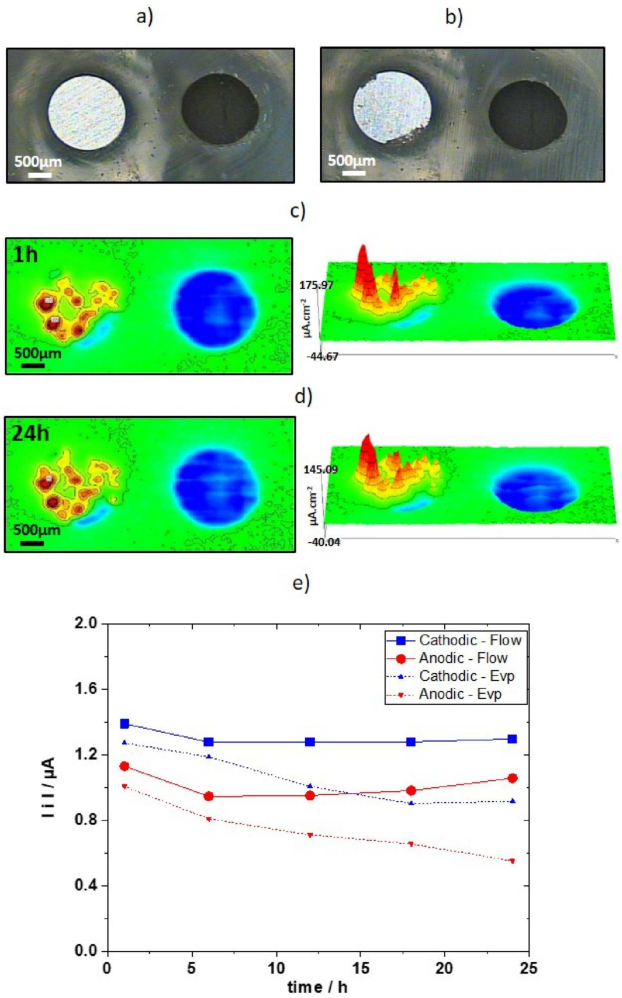

Fig. 8. Repetition of the experiment presented in Figure 1 with the recirculating flow system with peristaltic pump. a) optical micrograph of the CFRP-AA2024 couple after 1 h of immersion, b) optical micrograph after 24 h of immersion, c) SVET maps of current density measured 100 µm above the surface after 1 hour; d) SVET maps measured after 24 hours ;e) integrated cathodic and anodic current values at different periods of time (1 h, 6 h, 12 h, 18 h and 24 h) indicated in solid lines and highlighted in legend by "Flow". For comparison, dashed lines show the results presented in Figure 1g) obtained with spontaneous evaporation of solvent and highlighted as well in the legend by "Evp"

recirculating flow system of the electrolyte, in the course of the entire measurement.

Acknowledgements

This work was realized thanks to a partial financial support from European FP7 project "PROAIR" (PIAPP-GA-2013-612415) and Horizon 2020 project "MULTI-SURF" (Marie Skłodowska-Curie grant agreement No 645676). This work was also developed within the scope of the project CICECO-Aveiro Institute of Materials, FCT Ref. UID/CTM/50011/2019, financed by Portuguese national funds through the FCT/MCTES.

References

[1] H. S. Isaacs, Y. Ishikawa, *J. Electrochem. Soc.* **1985**, *132*, 1288.
[2] H. S. Isaacs, *Corrosion.* **1987**, *43*, 594.
[3] K. Ogle, V. Baudu, B. L. Garrigues, X. Philippe, *J. Electrochem. Soc.* **2000**, *10*, 3654.
[4] D. A. Worsley, H. N. McMurray, J. H. Sullivan, I. P. Williams, *Corrosion.* **2004**, *60* (2004), 437.
[5] H. Ding, L. H. Hihara, *J. Electrochem. Soc.* **2005**, *152*, B161.
[6] A. M. Simoes, D. Battocchi, D. E. Tallman, G. P. Bierwagen, *Corros. Sci.* **2007**, *49*, 3838.
[7] A. Alvarez-Pampliega, S. V. Lamaka, M. G. Taryba, M. Madani, J. De Strycker, E. Tourwé, M. G. S. Ferreira, H. Terryn, *Electrochim. Acta.* **2012**, *61*, 107.
[8] R. S. Lillard, P. Marcus, F. Mansfeld, Scanning electrode techniques for investigating near-surface solution current densities, *Analytical Methods in Corrosion Science and Engineering*, Editors, p. 571, CRC Press, Taylor and Francis Group, Boca Raton (**2006**).
[9] M. B. Jensen, D. E. Tallman, Application of SECM to corrosion studies, in: *Electroanal. Chem.*, A. J. Bard, C. Zoski, Editors, p. 186, CRC Press, Taylor and Francis Group, Boca Raton (**2012**).
[10] V. Upadhyay, D. Battocchi, *Prog. Org. Coat.* **2016**, *99*, 365.
[11] H. Shi, E. H. Han, S. V. Lamaka, M. L. Zheludkevich, F. Liu, M. G. S. Ferreira, *Prog. Org. Coat.* **2014**, *77*, 765.
[12] M. F. Montemor, D. V. Snihirova, M. G. Taryba, S. V. Lamaka, A. I. Kartsonakis, A. C. Balaskas, *Electrochim. Acta.* **2012**, *60*, 31.
[13] H. Shi, L. Wu, J. Wang, F. Liu, E. H. Han, *Corros. Sci.* **2017**, *127*, 230.
[14] Scheffey, Pitfalls of the vibrating probe technique, and what to do about them, *Ionic Currents in Development-Progress in Clinical and Biological Researchn○ 210*, R. Nuccitelli, Editor, p. 3, A. R. Liss Inc., New York (**1986**)
[15] H. S. Isaacs, *Corrosion.* **1990**, *46*, 677.
[16] H. S. Isaacs, *J. Electrochem. Soc.* **1991**, *138*, 722.
[17] H. N. McMurray, D. Williams, D. A. Worsley, *J. Electrochem. Soc.* **2003**, *150*, B567.
[18] S. V. Lamaka, M. Taryba, M. F. Montemor, H. S. Isaacs, M. G. S. Ferreira, *Electrochem. Commun.* **2011**, *13*, 20.
[19] R. Akid, M. Garma, *Electrochim. Acta.* **2004**, *49*, 2871.
[20] F. Thébault, B. Vuillemin, R. Oltra, K. Ogle, C. Allely, *Electrochim. Acta.* **2008**, *53*, 5226.
[21] B. P. Wilson, J. R. Searle, K. Yliniemi, D. A. Worsley, H. N. McMurray, *Electrochim. Acta.* **2012**, *66*, 52.
[22] A. S. Demeter, O. Dolgikh, A. C. Bastos, D. Deconinck, S. Lamaka, V. Topa, J. Deconinck, *Electrochim. Acta. 127* (**2014**) 45–52.
[23] A. C. Bastos, M. C. Quevedo, M. G. S. Ferreira, *Corros. Sci.* **2015**, *92*, 309.
[24] O. Dolgikh, A. S. Demeter, S. V. Lamaka, M. Taryba, A. C. Bastos, M. C. Quevedo, J. Deconinck, *Electrochim. Acta.* **2016**, *203*, 379.
[25] A. C. Bastos, M. C. Quevedo, O. V. Karavai, M. G. S. Ferreira, J. Electrochem. Soc. 2017, *164*, C973.
[26] L. B. Coelho, M. G. Olivier, *Corros. Sci.* **2018**, 136, 292.
[27] C. V. Ossia, C. U. Orji **2016**, *4*, 71.
[28] M. Yan, V. J. Gelling, B. R. Hinderliter, D. Battocchi, D. E. Tallman, G. P. Bierwagen, *Corros. Sci.* **2010**, *52*, 2636.
[29] A. S. Gnedenkov, S. L. Sinebryukhov, D. V. Mashtalyar, S. V. Gnedenkov, *Corros. Sci.* **2016**, *102*, 269.
[30] T. Hu, H. Shi, D. Hou, T. Wei, S. Fan, F. Liu, E. H. Han, *Appl. Surf. Sci.* **2019**, *467*,1011.

[31] Y. Wu, X. Zhu, W. Zhao, Y. Wang, C. Wang, Q. Xue, *J. Alloy. Comp.* **2019**, *777*, 135.
[32] H. Shi, E. Han, F. Liu, T. Wei, Z. Zhu, D. Xua, *Corros. Sci.* **2015**, *98*,150.
[33] P. Visser, M. Meeusen, Y. Gonzalez-Garcia, H. Terryn, J. M. C. Mol, *J. Electrochem. Soc.* **2017**, *164*C396.
[34] M. Serdechnova, M. Mohedano, B. Kuznetsov, C. L. Mendis, M. Starykevich, S. Karpushenkov, M. L. Zheludkevich, *J. Electrochem. Soc.* **2017**, *164*, C36.
[35] J. M. Falcón, L. M. Otubo, I. V. Aoki, *Surf. Coat. Technol.* **2016**, *303*, 319.
[36] M. Yan, V. J. Gelling, B. R. Hinderliter, D. Battocchi, D. F. Tallman, G. P. Bierwagen, *Corros. Sci.* **2010**, *52*, 2636.
[37] N. Jadhav, C. A. Vetter, V. J. Gelling, *Electrochim. Acta* **2013**, *102*, 28.
[38] Applicable Electronics, Inc. US. http://www.applicableelectronics.com/, (accessed 19 december **2018**).
[39] Science Wares, Inc. US. http://www.sciencewares.com/, (accessed 19 december **2018**) .
[40] P. F. Hammond, R. Goslin, *Ecology.* **1933**, *14*, 411.
[41] K. Hisatake, S. Tanaka, Y. Aizawa, *J. Appl. Phys.* **1993**, *73*, 7395.
[42] A. J. Bard, L. R. Faulkner, Fundamentals and Applications. Electrochemical Methods, p. *482*, Wiley, New York (**2001**).
[43] W. M. Haynes, *CRC Handbook of Chemistry and Physics*, CRC Press, Cleveland (**2014**).
[44] P. A. White, A. E. Hughes, S. A. Furman, N. Sherman, P. A. Corrigan, M. A. Glenn, D. Lau, S. G. Hardin, T. G. Harvey, J. Mardel, T. H. Muster, S. J. Garcia, C. Kwakernaak, J. M. C. Mol, *Corros. Sci.* **2009**, *51*, 2279.
[45] S. V. Lamaka, J. Gonzalez, D. Mei, F. Feyerabend, R. Willumeit-Römer, M. L. Zheludkevich, *Adv. Mater. Interfaces* **2018**, *18*, 1800169

Received: July 12, 2019
Accepted: August 7, 2019
Published online on August 22, 2019

